PRODUCTION OF PROMPT ELECTRONS IN THE CHARM P_t REGION AT $\sqrt{s}$=630 GeV

O. BOTNER [a], L.O. EEK [a], T. EKELÖF [b,a], K. FRANSSON [a], A. HALLGREN [b,a], P. KOSTARAKIS [b,c], G. LENZEN [d] and B. LUND-JENSEN [a]

[a] *University of Uppsala, S-751 21 Uppsala, Sweden*
[b] *CERN, CH-1211 Geneva 23, Switzerland*
[c] *Nuclear Research Centre Demokritos, GR-15310 Athens, Greece*
[d] *University of Wuppertal, D-5600 Wuppertal, FRG*

Received 7 July 1989

The production of prompt electrons at $\sqrt{s}=630$ GeV has been measured in the p_t range 0.5–2.0 GeV/c and the pseudorapidity range 1.1–1.7, using a ring imaging Cherenkov (RICH) counter installed in the UA2 experiment at the CERN p$\bar{p}$ collider. From our measurement of the electron/hadron ratio in the p_t range 0.9–1.5 GeV/c we conclude that the total charm production cross section at $\sqrt{s}=630$ GeV does not exceed 1.9 mb at 95% CL. As our best estimate we obtain $\sigma_{tot}(c\bar{c})=0.68\pm0.56$(stat.)$\pm0.25$(sys., exp.)$\pm0.21$(sys., theory) mb.

We report results from a measurement of the electron to charged hadron (e/h) ratio at $\sqrt{s}=630$ GeV in the p_t range 0.5–2 GeV/c, where the semi-leptonic decay of charm is expected to be the dominant source of prompt electrons. The measurements were carried out at the CERN p$\bar{p}$ collider with a ring imaging Cherenkov (RICH) counter [1] for electron identification and a two-plane scintillator hodoscope for triggering and track selection installed in the UA2 detector [2]. This is the first experiment in which a RICH counter has been used at a collider. Fig. 1a shows the experimental lay-out, with the RICH installed in one of the twelve azimuthal end-cap sectors of UA2, down-stream with respect to the proton beam. The RICH counter covers the polar angle region 20°–37.5°, corresponding to a pseudorapidity range 1.1–1.7, and an azimuthal range of 24°.

A closer view of the RICH counter is shown in fig. 1b, which illustrates how the photons radiated by a traversing electron are reflected by the spherical mirror (focal length 600 mm) to form a ring-image in the TPC-type single-photon position detector. The radiator volume is filled with the freon C_2F_6 at atmospheric pressure, implying a π threshold momentum of 3.5 GeV/c.

The π rejection power of the RICH counter was measured in a test beam at the CERN PS [3] where two 4 m long threshold Cherenkov counters were placed in front of the RICH for electron identification. The probability that an incoming electron would be misidentified as a pion by this system (i.e. lack of signal in both counters) was less than 2×10^{-7}. Fig. 2 shows the measured probability of misidentifying a pion as an electron in the RICH as a function of the beam momentum, for an electron identification efficiency of 48% (closed circles). In the analysis of the UA2 RICH data the rejection was improved by a factor of 10 by requiring that the candidate electron track should be isolated from other particles and have an energy deposition in the UA2 electromagnetic calorimeter characteristic of a single electron. In total we get, below the Cherenkov π threshold 3.5 GeV/c, a probability to misidentify a pion as an electron smaller than 10^{-5} (open circles) for a combined electron identification efficiency of 42%. The π rejection grows worse for momenta above the threshold. In the analysis of the UA2 RICH data we therefore imposed the cut $p<4$ GeV/c. We estimate that with our analysis criteria the contribution from misidentified hadrons to the e/h ratio in the p_t range 1.5–2 GeV/c is at most 1×10^{-4}. For $p_t<1.5$ GeV/c the

0370-2693/90/$ 03.50

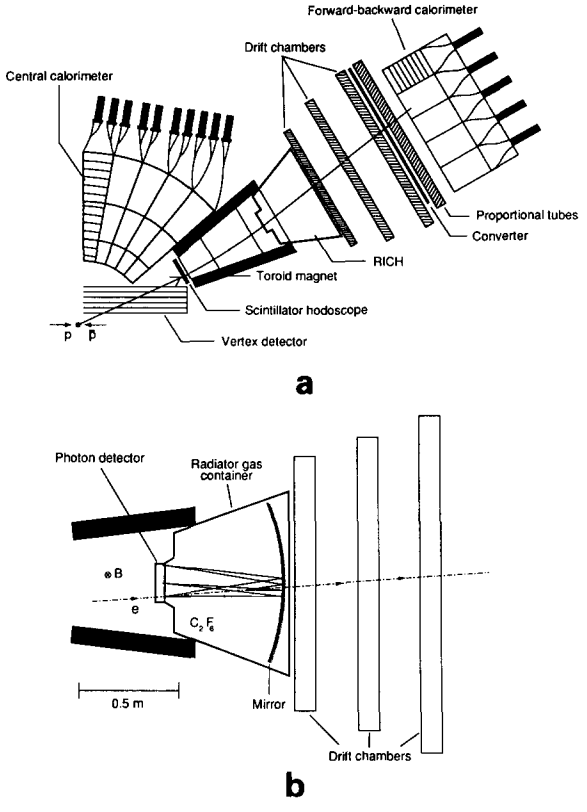

Fig. 1. (a) A schematic cross section of one quadrant of the UA2 experiment showing the position of the RICH counter. The outgoing track traverses, in succession, a cylindrical vertex detector (drift chambers and MWPC's) in a region with no magnetic field, the scintillator hodoscope, a toroidal magnetic field, the RICH counter, three planar drift chambers, a lead-iron converter (thickness 1.4 radiation lengths) followed by a proportional tube array (not used in this experiment), and enters finally an electromagnetic calorimeter, divided longitudinally into two compartments (24 and 6 radiation lengths, respectively) for better electron/hadron separation. Reconstruction tracks in the vertex detector determine the event vertex which in association with hits in the three planar drift chambers is used to measure charged particle momenta. (b) Cross section of the RICH counter in the UA2 showing the photon detector, the spherical mirror and the radiator-gas container.

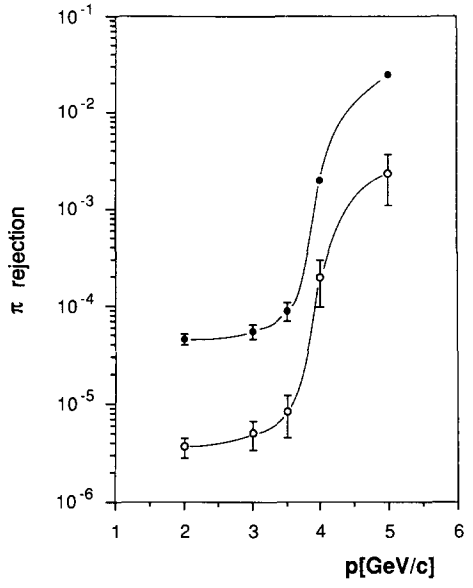

Fig. 2. The measured probability for misidentifying a pion as an electron, as a function of the particle momentum, using: the RICH counter alone: closed circles, the RICH counter combined with the calorimeter: open circles.

Table 1
Integrated luminosity and collected number of triggers.

Nominal trigger threshold [GeV]	$\int L\,dt$ [μb^{-1}]	Number of triggers
–	7.83	0.06×10^6
0.8	1660	0.6×10^6
1.4	2720	0.35×10^6

contribution is less than 9×10^{-6} and can be neglected.

Data with the RICH counter mounted in the UA2 set-up were collected during the autumn of 1985. The electron trigger required signals in both scintillator-hodoscope planes, in coincidence with signals obtained from "forward" scintillators close to the beam on both sides of the collision region. The forward scintillators gave a coincidence signal in more than 98% of all non-diffractive collisions [4]. In addition, the transverse energy deposition measured by the electromagnetic calorimeter behind the RICH, was required to be above a certain threshold. Two different trigger thresholds, 0.8 and 1.4 GeV, were used. Minimum bias triggers without any requirements on the calorimeter energy were recorded simultaneously, providing a sample of hadrons for normalization purposes. The integrated luminosities for the three data samples are indicated in table 1.

The data were processed through the UA2 track-fitting and calorimeter-shower reconstruction pro-

grams. The fitted tracks were then extrapolated to the RICH where an attempt was made to reconstruct a Cherenkov ring at the position predicted for the track. During further analysis a number of conditions were imposed on all three data samples:

(1) Event selection requirements:

– One single reconstructed track in the RICH sector, with segments measured by the vertex chamber as well as by the drift chambers behind the toroidal magnet, and with signals in the first two layers of the vertex chamber,

– a good track fit with a χ^2 corresponding to a probability of the momentum fit better than 0.01, and with momentum less than 4 GeV/c,

– pulse height in both scintillator-hodoscope planes in the range 0.5–1.35 times minimum ionization, i.e. consistent with that expected for a single, minimum-ionizing particle and significantly lower than that expected for two such particles, and

– the scintillator-hodoscope signal spatially associated with the track.

These criteria applied in the analysis of the minimum bias sample selected a set of 760 events, each containing a charged hadron in the p_t range 0.5–2 GeV/c.

To indentify events with prompt electron candidates the following additional requirements were imposed on the two data samples triggered on the electromagnetic calorimeter:

(2) Electron identification requirements:

–At most three "noise" signals in the RICH, a noise signal being defined as a signal which cannot be assigned to either a traversing track or to a Cherenkov ring,

– at least three photons detected within an annular region of width 20 mm centred at the position of the Cherenkov ring expected from the reconstructed track,

– the radius of the circle fitted to the detected photons consistent with 24 mm, as expected for a $\beta = 1$ particle,

– the energy deposition in the electromagnetic calorimeter equal to the measured momentum within 4σ and with a leakage into the hadronic compartment less than 2%, and

– no energy clusters in the calorimeter which cannot be assigned to the electron candidate.

The probability for a hadron to survive the electron identification cuts is indicated in fig. 2 (open circles) as a function of momentum. The electron identifications efficiency is a product of the following factors:

(a) Elimination of noisy events: 90%.

(b) At least three photons found: 77%.

(c) Fitted radius inside 24 ± 2 mm: 65%.

(d) Calorimeter requirement: 98%.

(e) Unassigned energy requirement: 95%.

All the efficiencies apart from (a) were estimated by Monte Carlo simulation. The inefficiency due to te RICH is caused by the requirement of at least three photons per Cherenkov ring when the average is 4.5 for a track traversing the full length of the radiator, and by the strict condition on the fitted radius (non-gaussian distribution with 3 mm FWHM). The response of the RICH was well reproduced by the Monte Carlo.

The criteria under point (1) reduced the two calorimeter-triggered event samples by a factor of about 800, the scintillator hodoscope requirement being very powerful in rejecting the abundant pairs of close tracks due to photon conversions. The criteria under point (2) resulted in a further reduction by a factor of about 60. The remaining 19 events were scanned visually to check the consistency of the detected images in the RICH. In one case ionization signals corresponding to two tracks traversing the RICH were observed – whereas only one track had been found in the drift chambers behind the RICH. This event was rejected. In four cases the ionization signals from a traversing track overlapped the ring image. With this event topology the probability of misidentifying a hadron is enhanced. The four events were therefore discarded. Prompt-electron events where the track overlaps the ring image do normally not survive the requirements under points (b) and (c). Therefore, rejecting the four events introduced only a negligible additional inefficiency. The final electron sample consisted of 14 events with equal numbers of electrons and positrons.

The true electron yield was obtained from this event sample by applying a calorimetertrigger acceptance-correction, calculated by means of a Monte Carlo program simulating the response of the electromagnetic calorimeter, and after correction for the electron identification efficiency discussed above. This yield was then normalized to the yield of charged hadrons in the same p_t range, obtained by analyzing

the minimum bias sample as described above. Since the analysis requirements based on information from the detectors common to both the electrons and the hadrons were imposed on all event samples, no further detection efficiency correction was needed to obtain the e/h ratio.

The measured e/h ratio is presented in table 2 for three momentum bins 0.5–0.9, 0.9–1.5 and 1.5–2.0 GeV/c, the first two corresponding to the calorimeter trigger with the lower nominal threshold and the last to the trigger with the higher threshold. The systematic errors presented in table 2 are due to uncertainties in the electron identification efficiency and in the calorimeter-trigger acceptance correction. The latter correction is particularly large for $p_t < 0.9$ GeV/c where the trigger acceptance varies rapidly with p_t.

To interpret the measured e/h ratio in terms of heavy-quark production the background contributions from trivial electron sources must be understood. The background comes mainly from electron–positron pairs generated by converting photons from the decays of neutral mesons (mostly π^0 and η). Other sources are the Dalitz decays of π^0 and η, the weak decays of charged and neutral kaons (K_{e3}) and Compton scattering.

In the first case the electron–positron pair has practically zero mass. Therefore, the conversion partner is likely to be found close to the presumed single-electron candidate. Such events are rejected in the analysis, partly by the single-track requirement and partly by the requirement that the pulse height measured by the scintillator hodoscope in front of the toroidal magnet be inconsistent with that for two charged tracks. Events with hits in the hodoscope which cannot be associated to the track segment downstream of the magnet are also discarded. Conversions occurring after the photon enters the vertex-chamber region are removed by requiring, for the candidate track, hits in the two inner vertex chambers. The difficult cases are those where one of the electrons is lost before the scintillator hodoscope due to multiple scattering. Many of these events are rejected using the calorimeter information since the second, non-converted photon deposits energy in the electromagnetic calorimeter.

The above methods eliminate most of the Dalitz decays as well. However, in this case the mass of the electron–positron pair is significantly different from zero which increases the probability for one of the partners escaping our solid angle before crossing the scintillator hodoscope.

The weak decays $K^{\pm} \to e^{\pm} + \pi^0 + \nu$ and $K_L^0 \to e^{\pm} + \pi + \nu$ produce single electrons which are difficult to distinguish from those originating from the processes $D^{\pm} \to e^{\pm} + X$ and $D^0 \to e^{\pm} + X$. The K_L^0 decays are removed is they occur outside the beam pipe by requiring for the candidate track hits in the two inner vertex chambers. The charged kaon decays are in most cases removed by the requirement of a good momentum fit for the candidate track, since this implies a track pointing at the interaction point.

The requirement of hits in the two inner vertex chambers also removes background from Compton scattering occurring outside the beam pipe.

The contribution to the e/h ratio from the residual background remaining after application of the above cuts (1) and (2) was calculated by Monte Carlo. The contribution form π^0's was computed using for the shape of the π^0 p_t-distribution the fit by UA2 [4] to the $p\bar{p} \to h + X$ data, since this extends to lower p_t values than the $p\bar{p} \to \pi^0 + X$ fit. The measured ratio $2\pi^0/(h^+ + h^-) = 0.68 \pm 0.13$ [4] was used to convert the

Table 2
Measured e/h, Monte Carlo calculated residual e/h from trivial background sources, and e/h after residual-background subtraction, in units of 10^{-4}. The error quoted are, respectively, statistical and systematic. In the case of the residual background, the errors have been added in quadrature.

p_t[GeV/c]	$\langle p_t \rangle$	No. of events	e/h($\times 10^4$)		
			measured	MC residual b.gr.	prompt e
0.5–0.9	0.6	4	$3.4 \pm 1.7 \pm 1.0$	4.5 ± 0.9	$-1.0 \pm 1.7 \pm 1.4$
0.9–1.5	1.1	7	$3.7 \pm 1.4 \pm 0.5$	1.7 ± 0.4	$2.0 \pm 1.4 \pm 0.6$
1.5–2.0	1.8	3	$7.2 \pm 4.1 \pm 1.0$	0.83 ± 0.26	$6.4 \pm 4.3 \pm 1.0$

residual background e/π^0 ratio into an e/h ratio. The contribution from η's was obtained using the same fit for the p_t-spectrum. The η/π^0 ratio was taken to be 0.6 ± 0.16 [4]. The K_{e3} and Compton contributions were calculated to be negligible compared to the contributions from π^0 and η conversions and Dalitz decays. Fig. 3 illustrates the variation with p_t of the dominant residual background contributions to the e/h ratio. All the cuts (1) and (2) have been applied. The systematic uncertainty on the sum of all the contributions is about 25%. The total residual background from π^0 and η conversions and Dalitz decays, expressed in terms of an e/h ratio, is given in table 2. THe quoted errors are mainly systematic.

As can be seen from table 2, the measured e/h in the p_t range 0.5–0.9 GeV/c is dominated by background. In the p_t range 0.9–1.5 GeV/c we get after background subtraction

$$e/h = [2.0 \pm 1.4(\text{stat.}) \pm 0.6(\text{sys.})] \times 10^{-4},$$

and in the range 1.5–2.0 GeV/c

$$e/h = [6.4 \pm 4.1(\text{stat.}) \pm 1.0(\text{sys.})] \times 10^{-4}.$$

The possible contribution from misidentified hadrons has been neglected. The systematic error of the measured value and that of the background have been added in quadrature.

The above e/h values may be converted into e/π using the π/h ratio of 0.68 ± 0.13. Including ± 0.13 in the systematic error we obtain for $0.9 < p_t < 1.5$

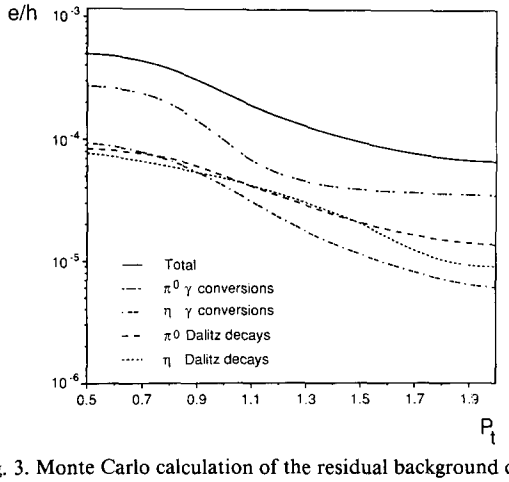

Fig. 3. Monte Carlo calculation of the residual background contributions to the e/h ratio as a function of p_t.

$$e/\pi = [3.0 \pm 2.1(\text{stat.}) \pm 1.3(\text{sys.})] \times 10^{-4},$$

and for $1.5 < p_t < 2.0$

$$e/\pi = [9.3 \pm 6.1(\text{stat.}) \pm 2.5(\text{sys.})] \times 10^{-4}.$$

From the e/h ratio we can compute an upper limit on the total charm production cross section by assuming that all our prompt electrons have this origin. We select the p_t range 0.9–1.5 GeV/c, where the dominant process contributing to the prompt electron yield is predicted to be the semi-leptonic decay of charmed particles and the contribution to the e/h from misidentified hadrons is negligible. For the p_t bin 1.5–2 GeV/c the background from misidentified hadrons is expected to be non-negligible. For this reason, and since the contributions from J/Ψ decays and semi-leptonic b-decays become increasingly important for $p_t > 1.5$ GeV/c, we choose not to consider these higher p_t. On the basis of the Monte Carlo calculation described below we expect that with our choice of p_t interval we should observe about 10% of the electron p_t spectrum from semi-leptonic charm decays within our solid angle. Taking into account the semi-leptonic branching ratios and our geometrical acceptance, this translates into about 0.01% of the total $c\bar{c}$ production cross section.

To describe charmed-particle production and semi-leptonic decay characteristics in our kinematical region, a Monte Carlo program has been used containing the quark–antiquark and gluon–gluon fusion processes to order α_s^2 [5]. In this program, the hadronization of the quarks and gluons follows the Lund string-model prescription [6]. This Monte Carlo was used to extrapolate our results to the full phase space and to correct for the restriction in decay topology imposed by the requirements of a single track in the RICH sector. After subtraction of background as described above and applying the Monte Carlo correction we obtain for the total charm production cross section the result

$$\sigma_{\text{tot}}(c\bar{c}) \leqslant 0.81 \pm 0.56(\text{stat.}) \pm 0.25(\text{sys., exp.})$$
$$\pm 0.24\ (\text{sys., theory})\ \text{mb}.$$

The second systematic error represents the uncertainty in the charm acceptance correction connected with the choice of the Lund Monte Carlo parameters.

Adding the different errors in quadrature the up-

per limit corresponding to a 95% confidence level is

$$\sigma_{tot}(c\bar{c}) < 1.9 \text{ mb} .$$

Assuming $\sigma(b\bar{b}) \approx 10$ μb [7] the contribution from semi-leptonic b decays to the prompt electron signal for $0.9 < p_t < 1.5$ was estimated to be 5%. Using the Pythia Monte Carlo program [8], the corresponding contribution from decays of the vector mesons ρ, ω, φ into e^+e^- was estimated to be about 10%. The absolute errors in these estimates are small in comparison to other errors. Neglecting them we obtain

$$\sigma_{tot}(c\bar{c}) = 0.68 \pm 0.56(\text{stat.}) \pm 0.25(\text{sys., exp.}) \pm 0.21(\text{sys., theory}) \text{ mb} .$$

Recently Nason et al. [9] have published results of a full calculation of the next-to leading order (α_s^3) QCD radiative corrections to the total cross section for heavy quark-pair hadroproduction. Based on these calculations Altarelli et al. [10] have evaluated the total charm cross section in pp collisions up to $\sqrt{s} = 63$ GeV. Fig. 4 shows the results of the same type of evaluation now extended to $\sqrt{2} = 630$ GeV [#1]. In this figure results from the measurements of the total charm production cross section in pp collisions at energies up to 63 GeV are plotted as well as our $p\bar{p}$ point at 630 GeV. The curves in fig. 4 correspond to different values of the charmed quark mass ($1.2 < m_c < 1.8$ GeV/c^2) and with different values of the Λ_5 parameter for the gluon structure function ($0.1 < \Lambda_5 < 0.25$ GeV). Because of the high $\sqrt{s}$ and the relatively low quark mass in our case, the cross section is sensitive to the behaviour of the structure functions in regions where no direct measurements exist so far. The value of the scale μ at which $\alpha_s(\mu)$ and the parton densities are calculated is set to 3 GeV. Using lower values for μ like $\mu \approx m_c = 1.5$ GeV decreases the $O(\alpha_s^2) + O(\alpha_s^3)$ cross sections at $\sqrt{s} = 630$ GeV by about a factor of 2. The significant dependence on the value chosen for μ indicates that even higher order corrections are important.

As compared to the $O(\alpha_s^2)$ calculations the introduction of the $O(\alpha_s^3)$ corrections more than doubles the cross section in the whole $\sqrt{s}$ range from 10 to 630 GeV. Our cross section at 630 GeV is consistent with the theoretical expectation although it is clear that within the present theoretical and experimental uncertainties no distinction between the various calculations can be made.

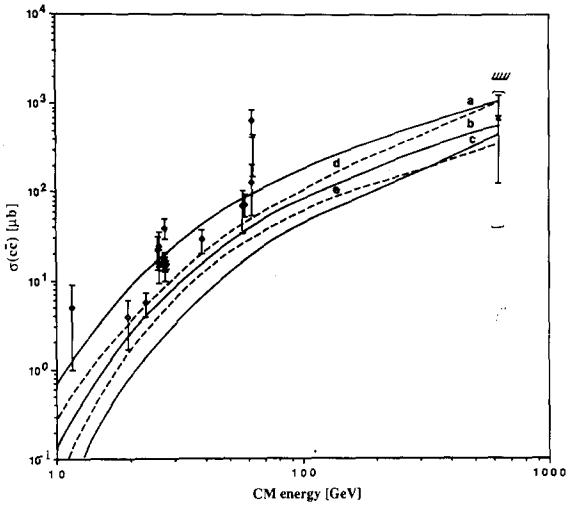

Fig. 4. $\sigma(c\bar{c})$ in hadroproduction. The open circles correspond to pp measurements [11]. Our $p\bar{p}$ result is marked with a cross and the upper limit corresponding to a 95% confidence level, assuming that all prompt electrons originate from charm decays, is indicated. The curves correspond to next-to-leading order QCD calculations (footnote 1) for pp collisions with the following parameters, using DFLM [12] structure-functions: a) $\Lambda_5 = 0.170$ GeV, $m_c = 1.2$ GeV/c^2; b) $\Lambda_5 = 0.170$, $m_c = 1.5$ GeV/c^2; c) $\Lambda_5 = 0.170$, $m_c = 1.8$ GeV/c^2; d) $\Lambda_5 = 0.250$, $m_c = 1.5$ GeV/c^2; e) $\Lambda_5 = 0.101$, $m_c = 1.5$ GeV/c^2. In all cases $\mu = 3$ GeV.

We thank the UA2 collaboration for having put their experimental set-up at our disposal. For their most helpful guidance in the use of the UA2 hardware and software we thank A. Clark, O. Gildemeister, R. Gregoire, J.R. Hansen and A. Sigrist. We thank T. Ypsilantis and J. Séguinot for their contribution to the development of the RICH counter, and A. Litke for his essential contributions in the intial stage of the experiment. We also wish to thank D. Bérnier, M. Bosteels, R. Bouhot, E. Lindholm, L. Mattsson, G. Muratori, C. Rivoiron, and G. Vismara for their realization of the various technical components of the RICH counter. The collaboration with G. Ingelman, G. Martinelli, and P. Nason for the theoretical calculations is gratefully acknowledged.

[#1] The calculations were made for us by P. Nason and G. Martinelli using the computer programs referred to in refs. [9,10].

References

[1] O. Botner et al., Nucl. Instrum. Methods A 257 (1987) 580; B. Lund-Hensen, Single-photon detectors for Cherenkov ring imgaging, Ph.D. Thesis, Uppsala University (1988).
[2] B. Mansoulié, Proc. 3rd Moriond Workshop on $p\bar{p}$ physics and the W discovery (La Plagne, 1983) (Editions Frontieres, Gif-sur-Yvette, 1983) p. 609, and references therein.
[3] L.O. Eek, Measurement of electron production in high-energy proton–antiproton collisions with a newly developed ring imaging Cherenkov counter, Ph.D. Thesis, Uppsala University (1989).
[4] M. Banner et al., Z. Phys. C 27 (1985) 329.
[5] G. Ingelman, Comput. Phys. Commun. 46 (1987) 217.
[6] B. Andersson, G. Gustafson, G. Ingelman and T. Sjöstrand, Phys. Rep. 97 (1983) 31;
T. Sjöstrand, Comput. Phys. Commun. 39 (1986) 347.
[7] UA1 Collab., C. Albajar et al., Phys. Lett. B 213 (1988) 405.
[8] H.U. Bengtsson and T. Sjöstrand, Comput. Phys. Commun. 46 (1987) 43.
[9] P. Nason et al., Nucl. Phys. B 303 (1988) 607.
[10] G. Altarelli et al., Nucl. Phys. B 308 (1988) 724.
[11] S.P.K. Tavernier, Rep. Prog. Phys. 50 (1987) 1439.
[12] M. Diemoz et al., Z. Phys. C 39 (1988) 21;
Charm Collab., J.V. Allaby et al., Phys. Lett. B 197 (1987) 281.